J|A|C|S
ARTICLES
Published on Web 01/24/2004

Theoretical Study of the Spin Trapping of Hydroxyl Radical by Cyclic Nitrones: A Density Functional Theory Approach

Frederick A. Villamena,*,† Christopher M. Hadad,*,‡ and Jay L. Zweier*,†

Contribution from the Center for Biomedical EPR Spectroscopy and Imaging, and The Davis Heart and Lung Research Institute, College of Medicine, and Department of Chemistry, The Ohio State University, Columbus, Ohio, 43210

Received October 2, 2003; E-mail: villamena-1@medctr.osu.edu; hadad.1@osu.edu; zweier-1@medctr.osu.edu

Abstract: The hydroxyl radical (•OH) is an important mediator of biological oxidative stress, and this has stimulated interest in its detection. 5,5-Dimethyl-1-pyrroline *N*-oxide (DMPO) and its alkoxycarbonyl and alkoxyphosphoryl analogues have been employed as spin traps for electron paramagnetic resonance (EPR) spectroscopic radical detection. Energies of optimized geometries of nitrones and their corresponding •OH adducts were calculated using density functional theory (DFT) at the B3LYP/6-31+G**//B3LYP/6-31G* level. Calculations predict that the *trans* adduct formation is favored in alkoxycarbonyl nitrones, while *cis* adducts with intramolecular H-bonding is favored for alkoxyphosphoryl nitrones. Addition of •OH to a phosphoryl-substituted nitrone is more exoergic than the carbonylated nitrones. Charge and spin densities on the nitrone spin traps were correlated with their rates of addition with •OH, and results show that the charge density on the nitronyl C, the site of •OH addition, is more positive in phosphorylated nitrones compared to DMPO and the alkoxycarbonyl nitrones. The dihedral angle between the β-H and nitroxyl O bonds is smaller in phosphorylated nitrones, and that aspect appears to account for the longer half-lives of the spin adducts compared to those in DMPO and alkoxycarbonyl nitrones. Structures of nitrones with trifluoromethyl-, trifluoromethylcarbonyl-, methylsulfonyl-, trifluoromethylsulfonyl-, amido-, spiropentyl-, and spiroester substituents were optimized and their energies compared. Amido and spiroester nitrones were predicted to be the most suitable nitrones for spin trapping of •OH due to the similarity of their thermodynamic and electronic properties to those of alkoxyphosphoryl nitrones. Moreover, dimethoxyphosphoryl substitution at C-5 was found to be the most efficient substitution site for spin trapping of •OH, and their spin adducts are predicted to be the most stable of all of the isomeric forms.

I. Introduction

Nitrones and the related nitroxides have emerged in recent years as versatile functional groups with a wide variety of applications. Nitrones, for example, are widely employed in 1,3-dipolar cycloaddition reactions[1] for natural product syntheses and in spin trapping of radicals for in vivo and in vitro applications.[2] Nitroxides have been used in enantioselective oxidation processes,[3] as biophysical probes and contrast agents in magnetic resonance spectroscopy,[4] in living radical polymerizations,[5] as spin labels,[6] and as molecular magnetic materials.[7]

Free radicals are thought to be involved in lipid peroxidation processes, DNA cleavage, and enzyme inactivation.[8−10] These oxidative damages can lead to various diseases, including ischemic and postischemic reperfusion cell damage.[11] Oxygen free radicals (OFR) and reactive oxygen species (ROS) are key mediators of heart damage in acute myocardial infarction and are of particular importance in ischemia−reperfusion injury. The role of reactive oxygen species (ROS) such as hydroxyl (•OH) or superoxide ($O_2^{\bullet-}$) radicals in physiological and pathological processes has been extensively studied.[10]

In biological tissues, •OH or $O_2^{\bullet-}$ radicals are formed by a variety of specific molecular and cellular mechanisms.[12] These pathways are activated under different disease conditions. Fenton chemistry, ionizing radiation, lithotripsy, and ultrasonication are also some of the pathways in which •OH radicals can be generated.[10] Failure to eliminate these active species sometimes leads to cellular injury. To understand biological mechanisms involving free radicals requires efficient radical trapping and their accurate characterization. The specific detection of radicals

† Center for Biomedical EPR Spectroscopy and Imaging and The Davis Heart and Lung Research Institute, College of Medicine.
‡ Department of Chemistry.

(1) Jones, R. C. F.; Martin, J. N. *Chem. Heterocycl. Compd.* **2002**, *59*, 1−81.
(2) Janzen, E. G.; Haire, D. L. *Adv. Free Radical Chem.* **1990**, *1*, 253−295.
(3) Naik, N.; Braslau, R. *Tetrahedron* **1998**, *54*, 667−696.
(4) Swartz, H. M. *Bull. Magn. Reson.* **1986**, *8*, 172−175.
(5) Hawker, C. J.; Bosman, A. W.; Harth, E. *Chem. Rev.* **2001**, *101*, 3661−3688.
(6) Berliner, L. J. In *Spectroscopy in Biochemistry*; Bell, J. E., Ed.; CRC: Boca Raton, Fla, 1981; Vol. 2, pp 1−56.
(7) Kawakami, T.; Yamanaka, S.; Mori, W.; Yamaguchi, K.; Kajiwara, A.; Kamachi, M. *Chem. Phys. Lett.* **1995**, *235*, 414−421.
(8) Lai, C.; Piette, L. H. *Biochem. Biophys. Res. Commun.* **1977**, *78*, 51−59.
(9) Roberfroid, M.; Calderon, P. B. *Free Radicals and Oxidation Phenomena in Biological Systems*; Mercel Dekker: New York, 1995.
(10) Halliwell, B.; Gutteridge, J. M. C. *Free Radicals in Biology and Medicine*; Oxford Univeristy Press: Oxford, 1999.
(11) Bilenko, M. V. *Ischemia and Reperfusion of Various Organs: Injury, Mechanisms, Methods of Prevention and Treatment*; Nova Science Pub. Inc.: Huntington, New York, 2001.
(12) Suzuki, Y. J.; Forman, H. J.; Sevanian, A. *Free Radical Biol. Med.* **1997**, *22*, 269−285.

10.1021/ja038838k CCC: $27.50

Scheme 1

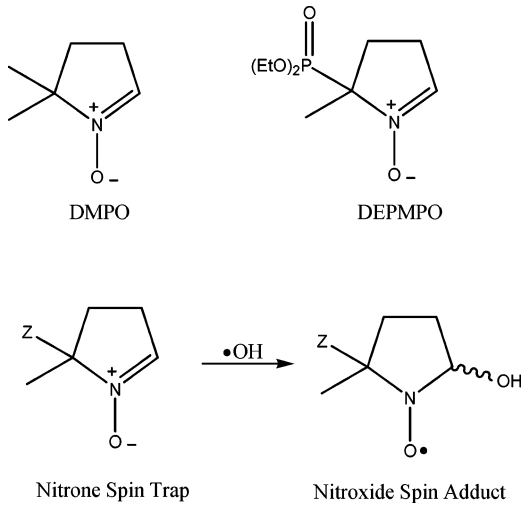

generated from biological processes relies mostly on electron paramagnetic resonance (EPR) spin trapping methods (Scheme 1) utilizing the nitrone spin traps 5,5-dimethyl-1-pryrroline *N*-oxide (DMPO) and 5-diethoxyphosphoryl-5-methyl-1-pyrroline *N*-oxide (DEPMPO).[13−17]

The spin-trapping technique has also found application in the study of kinetics and mechanisms of certain organic reactions,[18−21] sonolysis,[22] lipid peroxidation,[23−25] smoke toxicity,[26] Fenton-type reactions,[27,28] and *in vivo* and in vitro enzymatic reactions.[13−15,29] It has been more than four decades now since DMPO was first synthesized,[30] and its ability to trap radicals has been observed by EPR spectroscopy by Janzen[31] and Iwamura.[32] Although a variety of both DMPO- and phenyl-*tert*-butyl nitrone (PBN)-type nitrones have surfaced since these earlier reports, the application of these spin traps to investigate radical formation in biological systems still faces several limitations. Among these limitations are the following: (1) the inefficiency of certain nitrones to trap particular types of radicals, (2) an inability to discern from the EPR spectral profile of the spin adducts as to which radical is being trapped, for example $O_2^{\bullet-}$ vs •OH, or $\bullet CH_3$ vs $\bullet CH_2CH_3$, (3) the short persistence of the spin adducts, for example the superoxide radical adduct of DMPO rapidly decomposes to the •OH adduct,[33] and (4) the lack of chemical availability, the difficulty of purification and the cytotoxicity of some of the nitrone spin traps.

The need to correlate the reactivity of spin traps and the stability of their spin adducts with electronic properties, as well as to determine thermodynamic and kinetic parameters from theoretical calculations, would be valuable in the development of future spin traps with improved properties. We previously demonstrated qualitatively that theoretical data derived from semiempirical and Hartree−Fock (HF) methods can be correlated with experimental kinetic data.[34,35] Earlier theoretical studies were focused on the energetics of spin trapping by nitrosomethane[36] and simple alkyl nitrones[37] using HF and second-order Møller−Plesset (MP2) levels of theory. The most recent study[38] on PBN-type nitrones demonstrated that the addition of methyl radical to the nitrone is more favored both thermodynamically and kinetically than proton abstraction from nitrones. However, the effect of substituents on the geometry and the electronic and thermodynamic properties of DMPO-type nitrones as well as their corresponding spin adducts has not received much attention.

Recently, ethoxycarbonyl-5-methyl-1-pyrroline *N*-oxide (EMPO),[39,40] *tert*-butoxycarbonyl-5-methyl-1-pyrroline *N*-oxide (BocMPO),[34,41] (DEPMPO),[16,17] and 5-diispropyloxyphosphoryl-5-methyl-1-pyrroline *N*-oxide (DIPPMPO) have been reported to trap •OH and $O_2^{\bullet-}$. Their experimental kinetic parameters have also been described,[34,35] making all of them appropriate models for this theoretical investigation.

We now report a comprehensive theoretical analysis of DMPO-type nitrones, their corresponding •OH adducts, and their spin-trapping reaction with •OH using density functional theory (DFT) with the aim of introducing a new approach in the development of more efficient spin traps with longer spin adduct half-life.

II. Computational Methods

Density functional theory[42,43] was applied in this study to determine the optimized geometry, vibrational frequencies, and single-point energy of all stationary points.[44−47] All calculations were performed using Gaussian 98[48] at the Ohio Supercomputer Center or using Gaussian 98W (for Windows).[48] Single-point energies were obtained at the B3LYP/6-31+G** level based on the optimized B3LYP/6-31G*

(13) Zweier, J. L.; Kuppusamy, P.; Williams, R.; Rayburn, B. K.; Smith, D.; Weisfeldt, M. L.; Flaherty, J. T. *J. Biol. Chem.* **1989**, *264*, 18890−18895.
(14) Zweier, J. L.; Kuppusamy, P.; Lutty, G. A. *Proc. Natl. Acad. Sci. U.S.A.* **1988**, *85*, 4046−4050.
(15) Zweier, J. L.; Flaherty, J. T.; Weisfeldt, M. L. *Proc. Natl. Acad. Sci. U.S.A.* **1987**, *84*, 1404−1407.
(16) Roubaud, V.; Sankarapandi, S.; Kuppusamy, P.; Tordo, P.; Zweier, J. *Anal. Biochem.* **1998**, *254*, 210−217.
(17) Roubaud, V.; Sankarapandi, S.; Kuppusamy, P.; Tordo, P.; Zweier, J. L. *Anal. Biochem.* **1997**, *247*, 404−411.
(18) Rojas Wahl, R. U.; Zeng, L.; Madison, S. A.; DePinto, R. L.; Shay, B. J. *J. Chem. Soc., Perkin Trans. 2* **1998**, 2009−2017.
(19) Jenkins, C. A.; Murphy, D. M.; Rowlands, C. C.; Egerton, T. A. *J. Chem. Soc., Perkin Trans. 2* **1997**, 2479−2485.
(20) Santos, C. X. C.; Anjos, E. I.; Ohara, A. *Arch. Biochem. Biophys.* **1999**, *372*, 285−294.
(21) Hawkins, C. L.; Davies, M. J. *Free Radical Biol. Med.* **1998**, *24*, 1396−1410.
(22) Misik, V.; Reisz, P. *Ultrason. Sonochem.* **1996**, *3*, S173−S186.
(23) Stolze, K.; Udilova, N.; Nohl, H. *Free Radical Biol. Med.* **2000**, *29*, 1005−1014.
(24) Dikalov, S. I.; Mason, R. P. *Free Radical Biol. Med.* **2001**, *30*, 187−197.
(25) Lai, C.; Piette, L. H. *Biochem. Biophys. Res. Commun.* **1977**, *78*, 51−59.
(26) Zhang, L.-Y.; Stone, K.; Pryor, W. A. *Free Radical Biol. Med.* **1995**, *19*, 161−167.
(27) Ma, Z.; Zhao, B.; Yuan, Z. *Anal. Chim. Acta* **1999**, *389*, 213−218.
(28) Gianni, L.; Zweier, J.; Levy, A.; Myers, C. E. *J. Biol. Chem.* **1985**, *260*, 6820−6826.
(29) Sankarapandi, S.; Zweier, J. *J. Biol. Chem.* **1999**, *274*, 34576−34583.
(30) Bonnett, R.; Clark, V. M.; Giddy, A.; Todd, A. *J. Chem. Soc.* **1959**, 2087−2093.
(31) Janzen, E. G.; Blackburn, B. J. *J. Am. Chem. Soc.* **1968**, *90*, 5909−5910.
(32) Iwamura, M.; Inamoto, N. *Bull. Chem. Soc. Jpn.* **1967**, *40*, 703.
(33) Buettner, G. R.; Oberley, L. W. *Biochim. Biophys. Acta* **1978**, *808*, 235−242.
(34) Villamena, F.; Zweier, J. *J. Chem. Soc., Perkin Trans. 2* **2002**, 1340−1344.
(35) Villamena, F.; Hadad, C. M.; Zweier, J. *J. Phys. Chem. A* **2003**, *107*, 4407−4414.
(36) Bentley, J.; Madden, K. P. *J. Am. Chem. Soc.* **1994**, *116*, 6, 11397−11406.
(37) Boyd, S. L.; Boyd, R. J. *J. Phys. Chem.* **1994**, *98*, 11705−11713.
(38) Boyd, S. L.; Boyd, R. J. *J. Phys. Chem. A* **2001**, *105*, 7096−7105.
(39) Zhang, H.; Joseph, J.; Vasquez-Vivar, J.; Karoui, H.; Nsanzumuhire, C.; Martasek, P.; Tordo, P.; Kalyanaraman, B. *FEBS Lett.* **2000**, *473*, 58−62.
(40) Olive, G.; Mercier, A.; Le Moigne, F.; Rockenbauer, A.; Tordo, P. *Free Radical Biol. Med.* **2000**, *28*, 403−408.
(41) Zhao, H.; Joseph, J.; Zhang, H.; Karoui, H.; Kalyanaraman, B. *Free Radical Biol. Med.* **2001**, *31*, 599−606.
(42) Labanowski, J. W.; Andzelm, J. *Density Functional Methods in Chemistry*; Springer: New York, 1991.
(43) Parr, R. G.; Yang, W. *Density Functional Theory in Atoms and Molecules*; Oxford University Press: New York, 1989.
(44) Becke, A. D. *Phys. Rev.* **1988**, *38*, 3098−3100.
(45) Lee, C.; Yang, W.; Parr, R. G. *Phys. Rev. B* **1988**, *37*, 785−789.
(46) Becke, A. D. *J. Chem. Phys.* **1993**, *98*, 1372.
(47) Hehre, W. J.; Radom, L.; Schleyer, P. V.; Pople, J. A. *Ab Initio Molecular Orbital Theory*; John Wiley & Sons: New York, 1986.

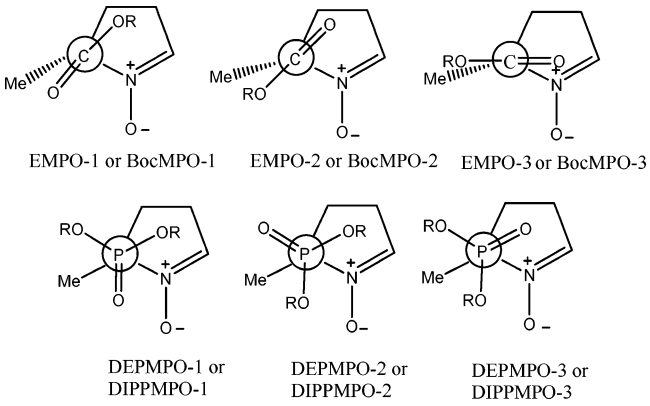

Figure 1. Conformers of various spin traps.

Scheme 2

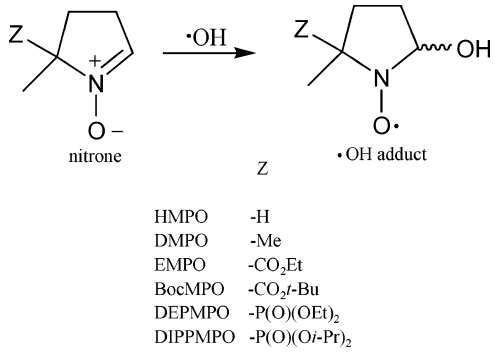

geometries. Stationary points for both the nitrone spin traps and •OH adducts have no imaginary vibrational frequencies as derived from a vibrational frequency analysis (B3LYP/6-31G*). A scaling factor of 0.9806 was used[49] for the zero-point vibrational energy (ZPE) corrections. Attempts to locate transition states were unsuccessful despite all attempts, and this was due to the strongly exothermic formation of products in the reactions (see below). Spin contamination for all of the stationary points for the •OH adduct radical structures was negligible, i.e., $0.75 < \langle S^2 \rangle < 0.76$. All spin and charge densities were obtained from natural population analysis (NPA) at the B3LYP/6-31G* level.[50] Experimental details of the kinetics of •OH trapping and adduct decay are provided elsewhere.[35]

III. Naming System

Acronyms of the nitrone spin traps used in this study and their corresponding hydroxyl adducts are shown in Scheme 2. The approximate conformations of the nitrones with alkoxycarbonyl (EMPO and BocMPO) and alkoxyphosphoryl (DEPMPO and DIPPMPO) groups are shown in Figure 1. Three possible conformations were used for both the alkoxycarbonyl and alkoxyphosphoryl nitrones.

Two configurations, i.e., *cis* and *trans* isomers, were assigned for the •OH adducts indicating the position of the alkoxycarbonyl and alkoxyphosphoryl substituents relative to the hydroxyl group (Figure 2). Each of the configurations of the •OH adduct has three conformations corresponding to their respective nitrone. In some adducts, calculations were performed on the *cis*-3 isomers in the presence and absence of intramolecular H-bonding.

Table 1. Comparison of Selected X-ray Crystallographic Bond Lengths with Calculated Bond Lengths (B3LYP/6-31G*)

bonds	calculated bond distances range[a] (Å)	experimental bond distances (Å)
nitronyl C═N	1.30−1.31	1.291(2);[53] 1.307(2)[51]
nitronyl N−O	1.25−1.27	1.2987(16);[53] 1.294(1)[51]
nitroxyl C−N	1.47−1.49	1.50[52]
nitroxyl N−O	1.27−1.28	1.27[52]
P═O	1.47−1.49	1.4636(12);[53] 1.458(2)[69]
P−OR	1.59−1.62	1.580(1);[53] 1.575(2)[69]
P−C	1.80−1.88	1.8276(16);[53] 1.813(3)[69]
C═O	1.20−1.22	1.233(5)[70]
C(O)-OR	1.33−1.35	1.358(5)[70]
C(O)-C	1.53−1.56	1.506(5)[70]
MeS═O(or CF_3S═O)	1.46−1.47	1.435(2)[71](1.418(1))[72]
S−CH_3	1.81−1.82	1.755(3)[71]
S−CF_3	1.89−1.92	1.850(1)[72]
SO_2−C	1.89−1.93	1.833(2)[73]
C−CF_3	1.53−1.55	1.530(3)[74]

[a] For certain functional groups other than the nitronyl and nitroxyl groups, values are based on both nitrones and spin adducts.

IV. Examination of Optimized Geometries

Selected bond distances of the nitrone spin traps and their •OH adducts are shown in Table 1 based on the optimized geometries at the B3LYP/6-31G* level of theory. The bond distances for the C═N in nitrone spin traps, the C−N in spin adducts, and the N−O in both nitrones and nitroxides are in good agreement with reported values.[51−53] Optimized bond distances for selected atoms in alkoxyphosphoryl, alkoxycarbonyl, amido, sulfonyl, and carboxyl groups are in good agreement with the experimental results.

Intramolecular H-bonding between the OH group and the carbonyl or the phosphoryl oxygens is predicted in some of the spin adducts with a *cis* configuration (Figure 3). The O- - -H−O distances were calculated to be in the range of 1.874−2.078 Å with the shortest bond distance for the DIPPMPO−OH *cis*-3 isomer (Table 2). Initial structures with the C═O facing the H−O gave optimized structures in which the O- - -H−O distances were in the range of 2.04−2.06 Å.

Table 3 shows the dihedral ∠$\boldsymbol{C}H_3$−$\boldsymbol{C}$−$\boldsymbol{C}$═$\boldsymbol{O}$ for EMPO, BocMPO, TFCOMPO, AMPO, and SpiroCOMPO; ∠$\boldsymbol{C}H_3$−$\boldsymbol{C}$−$\boldsymbol{P}$═$\boldsymbol{O}$ for DEPMPO, DIPPMPO; ∠$\boldsymbol{C}H_3$−$\boldsymbol{C}$−$\boldsymbol{C}$−$\boldsymbol{C}$ for CPPO and TFMPO; and ∠$\boldsymbol{C}H_3$−$\boldsymbol{C}$−$\boldsymbol{S}$−$\boldsymbol{C}$ for MSMPO and TFSMPO, and all of their corresponding spin adducts based on the B3LYP/6-31G* optimized structures. Dihedral angles are in the range of 190−215° (Table 3) as found for *cis* isomers exhibiting intramolecular H-bonding. Attempts to optimize a structure for BocMPO-3 only resulted in a conformation similar to that of BocMPO-2 with negligible change in total energy of 0.02 kcal/mol.

(48) Frisch, M. J.; Trucks, G. W.; Schlegel, H. B.; Scuseria, G. E.; Robb, M. A.; Cheeseman, J. R.; Zakrzewski, V. G.; Montgomery, J. A., Jr.; Stratmann, R. E.; Burant, J. C.; Dapprich, S.; Millam, J. M.; Daniels, A. D.; Kudin, K. N.; Strain, M. C.; Farkas, O.; Tomasi, J.; Barone, V.; Cossi, M.; Cammi, R.; Mennucci, B.; Pomelli, C.; Adamo, C.; Clifford, S.; Ochterski, J.; Petersson, G. A.; Ayala, P. Y.; Cui, Q.; Morokuma, K.; Rega, N.; Salvador, P.; Dannenberg, J. J.; Malick, D. K.; Rabuck, A. D.; Raghavachari, K.; Foresman, J. B.; Cioslowski, J.; Ortiz, J. V.; Baboul, A. G.; Stefanov, B. B.; Liu, G.; Liashenko, A.; Piskorz, P.; Komaromi, I.; Gomperts, R.; Martin, R. L.; Fox, D. J.; Keith, T.; Al-Laham, M. A.; Peng, C. Y.; Nanayakkara, A.; Challacombe, M.; Gill, P. M. W.; Johnson, B.; Chen, W.; Wong, M. W.; Andres, J. L.; Gonzalez, C.; Head-Gordon, M.; Replogle, E. S.; Pople, J. A. *Gaussian 98*, revision A.11.3; Gaussian, Inc.: Pittsburgh, PA, 2002.
(49) Scott, A. P.; Radom, L. *J. Phys. Chem.* **1996**, *100*, 16502−16513.
(50) Reed, A. E.; Weinhold, F. A.; Curtiss, L. A. *Chem. Rev.* **1998**, *98*, 899.
(51) Villamena, F.; Dickman, M. H.; Crist, D. R. *Inorg. Chem.* **1998**, *37*, 1446−1453.
(52) Boeyens, J. C. A.; Kruger, G. J. *Acta Crystallogr.* **1970**, *B26*, 668.
(53) Xu, Y. K.; Chen, Z. W.; Sun, J.; Liu, K.; Chen, W.; Shi, W.; Wang, H. M.; Zhang, X. K.; Liu, Y. *J. Org. Chem.* **2002**, *67*, 7624−7630.

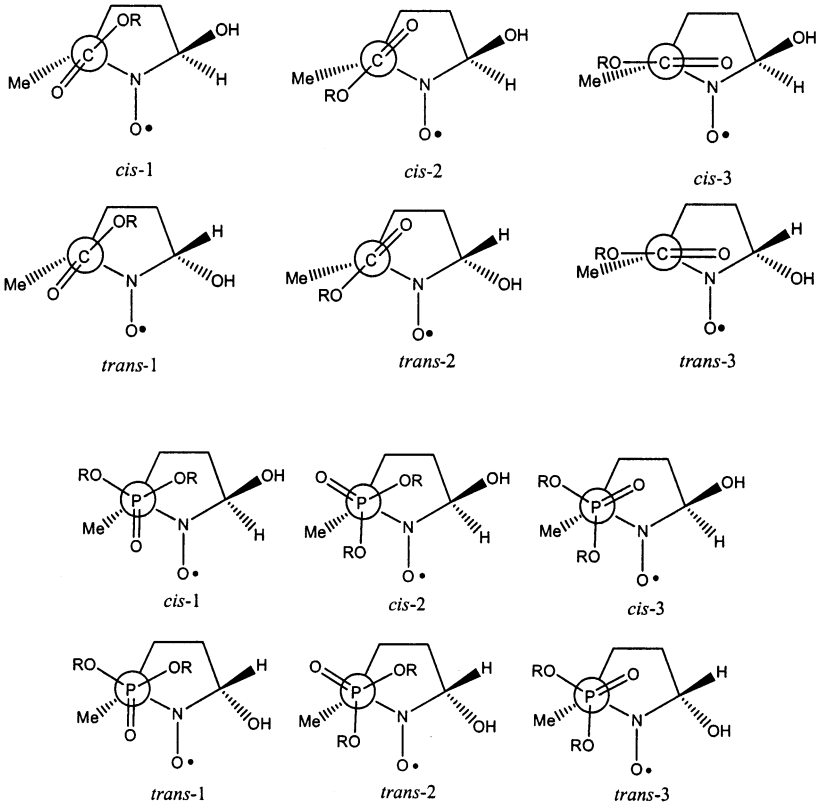

Figure 2. Conformational and configurational isomers of various hydroxyl spin adducts.

Table 2. Intramolecular Hydrogen Bond; O−H- - -O=C (or O−H- - -O=P) distances

spin adduct	bond distances (Å)
EMPO−OH cis 3	2.057
BocMPO−OH cis−3	2.038
DIPPMPO−OH cis 3	1.874
DEPMPO−OH cis 3	1.922
AMPO−OH *cis*	1.970
AMPO−OH *cis*[a]	2.045
AMPO−OH *trans*[a]	2.094
CPCOMPO−OH *cis*	2.016
TFCOMPO−OH *cis*	2.169
TFCOMPO−OH *cis*[b]	2.256
TFMPO−OH *cis*[b]	2.425
DMMPO-5-OH *cis*	1.952
DMMPO-3-OH *cis*	2.078

[a] N−H- - -O−N. [b] C−F- - -H−O.

V. Alkoxycarbonyl vs Alkoxyphosphoryl Substituents

V. A. Nitrones. Relative energies shown in Table 4 indicate that energy differences among conformers of alkoxycarbonyl nitrones, EMPO and BocMPO, are not as significant compared to those of alkoxyphosphoryl nitrones DEPMPO and DIPPMPO. For example, both EMPO and BocMPO gave relative energy differences of only 0.2 and 0.6 kcal/mol, respectively, with preference for conformer-2 in EMPO and conformer-1 in BocMPO consistent with the X-ray structure[54] as shown in Figure 4. However, relative energies among conformations in alkoxyphosphoryl nitrones are quite significant, namely ∼2.0 kcal/mol. In both DEPMPO and DIPPMPO nitrones, conformer-3 is the most preferred conformation consistent with X-ray structures reported by Tordo[55] for DIPPMPO and Liu[53] for 5-diethoxyphosphoryl-5-phenylethyl-1-pyrroline *N*-oxide (DEPPEPO), a close analogue of DEPMPO.

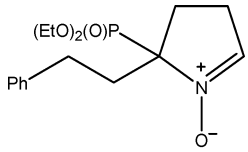

DEPPEPO

This most favored staggered conformation minimizes overcrowding of the alkyl substituents of the phosphoryl moiety with the nitrone ring. Calculated dipole moments (Table 4) are highest in conformer-1 for all of the substituted nitrones (∼4.5 D) comparable to that of the simple nitrones HMPO and DMPO with dipole moments of 4.03 and 3.72 D, respectively, while dipole moments of the most energetically favorable conformer-3 of DEPMPO and DIPPMPO are less polar with values of 3.36 and 3.24 D, respectively.

V. B. Nitroxides. Table 5 shows the relative energies of different configurational as well as conformational isomers of EMPO, BocMPO, DEPMPO, and DIPPMPO adducts with OH radical. Energy differences among the different isomeric forms of EMPO−OH and BocMPO−OH are smaller as compared to those of DEPMPO−OH and DIPPMPO−OH. The most favored configuration is *trans* for both •OH adducts of EMPO and BocMPO, but the total energy differences between the *trans* conformers have a range of only ca. 0.2 kcal/mol for both EMPO−OH and BocMPO−OH. Interestingly, the isomer *cis*-3

(54) BocMPO: $C_{10}H_{17}NO_3$, m., $P2(1)/n$, a = 12.1985(2) Å, b = 6.2722(1) Å, c = 14.5012(3) Å, = 107.039(1)°, V = 1060.81(3) Å^3; final R_1 = 0.037.

(55) Chalier, F.; Tordo, P. *J. Chem. Soc., Perkin Trans. 2* **2002**, 2110−2117.

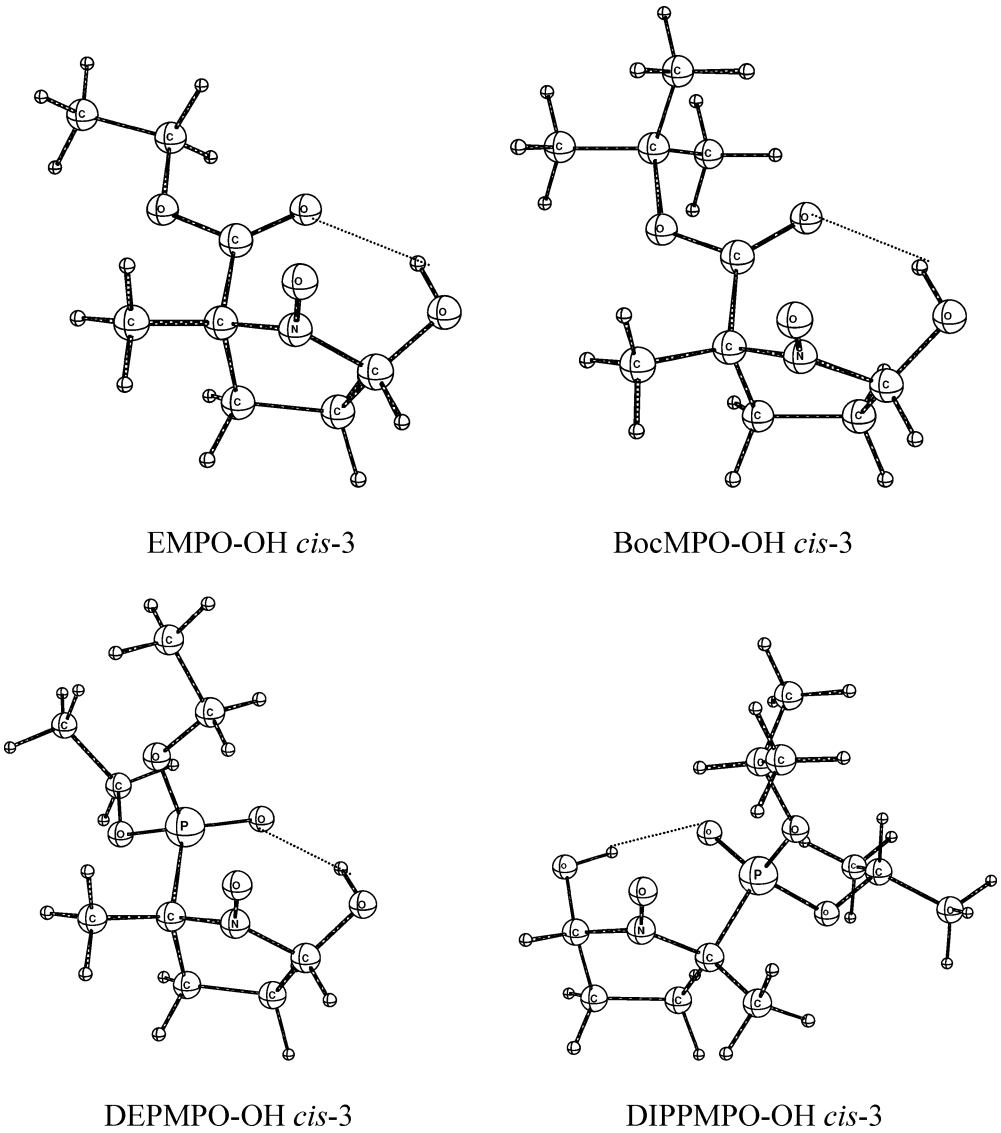

Figure 3. Hydroxyl radical adducts exhibiting intramolecular H-bonding in optimized structures at the B3LYP/6-31G* level of theory. Broken lines indicate sites of intramolecular H-bonding and their distances are shown in Table 2.

is the most preferred isomer for the •OH adducts with DEPMPO and DIPPMPO and with significant energy stabilization of 3.3 and 4.1 kcal/mol, respectively, relative to their *cis*-1 isomers. The total energy for DEPMPO−OH *cis*-3 conformation with intramolecular H-bonding is ca. 3.0 kcal/mol more than its *cis*-3 conformer without H-bonding. As mentioned earlier, these hydrogen bonds are relatively stronger in alkoxyphosphoryl substituted spin adducts compared to those in the alkoxycarbonyl •OH adducts (Table 2). The relative energies at the B3LYP/6-31+G**//B3LYP/6-31G** level for DEPMPO−OH *cis*-3 adducts in the presence and absence of intramolecular H-bonding were also calculated and compared with values at the fully optimized B3LYP/6-31+G**. Results show no significant difference in the relative bottom-of the-well energies as well as enthalpies of formation (see Supporting Information Table 5). Calculation at the CCSD(T)/6-31G*//B3LYP/6-31G* level of theory was not successful due to the size of the DEPMPO and its adduct. However, energies of formation at the CCSD(T)/6-31G*//B3LYP/6-31G* level of theory have been predicted for the DMPO−OH adduct and gave an $E_{0,\mathrm{rxn}} = -50.66$ kcal/mol compared to $E_{0,\mathrm{rxn}} = -50.70$ kcal/mol at the B3LYP/6-31+G**//B3LYP/6-31G* level, thereby further validating the theoretical method employed in this study (Supporting Information Table 6). The effect of solvation on the gaseous-phase calculations was also investigated using the polarized continuum model (PCM).[56−60] Energies of solvation range from −0.77 to 1.50 kcal/mol with greater than 2 kcal/mol preference for the formation of H-bonded DEPMPO−OH and DIPPMPO−OH adducts in aqueous environment (Supporting Information Table 7). Thus, solvation will only slightly perturb the relative energies as compared to the large exothermicities involved in the gas phase.

Despite the relatively weak intramolecular hydrogen bonding present in alkoxycarbonyl •OH adducts, their isomeric forms are not that thermodynamically favored. In general, the dipole moments are highest in conformations with intramolecular H-bonding (Table 5). Dipole moments for HMPO−OH (2.23

(56) Tomasi, J.; Persico, M. *Chem. Rev.* **1994**, *94*, 2027.
(57) Cossi, M.; Barone, V.; Cammi, R.; Tomasi, J. *Chem. Phys. Lett.* **1996**, *255*, 327.
(58) Barone, V.; Cossi, M.; Tomasi, J. *J. Chem. Phys.* **1997**, *107*., 3210.
(59) Barone, V.; Cossi, M.; Tomasi, J. *J. Comput. Chem.* **1998**, *19*, 404.
(60) Cossi, M.; Barone, V. *J. Chem. Phys.* **1998**, *109*, 6246.

Table 3. Dihedral Angles of ∠CH_3-*C*-*C*=*O*(or *P*=*O*) in Alkoxycarbonyl and Alkoxyphosphoryl Nitrones and Nitroxide

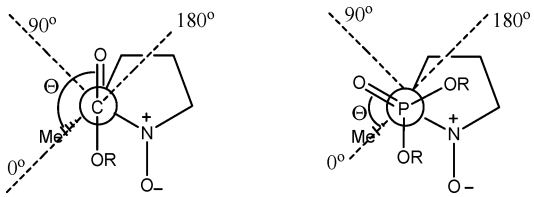

nitrone	Θ	*cis*-adduct	Θ	*trans*-adduct	Θ
EMPO-1	10.2	EMPO−OH 1	20.3	EMPO−OH 1	25.8
EMPO-2	168.3	EMPO−OH 2	129.4	EMPO−OH 2	133.5
EMPO-3	170.5	EMPO−OH 3	209.3[c]	EMPO−OH 3	209.0
BocMPO-1	12.1	BocMPO−OH 1	9.6	BocMPO−OH 1	17.7
BocMPO-2	160.3	BocMPO−OH 2	120.4	BocMPO−OH 2	133.7
BocMPO-3	160.2	BocMPO−OH 3	208.3[c]	BocMPO−OH 3	213.5
DEPMPO-1	327.9	DEPMPO−OH 1	323.4	DEPMPO−OH 1	324.2
DEPMPO-2	72.1	DEPMPO−OH 2	34.6	DEPMPO−OH 2	40.9
DEPMPO-3	188.0	DEPMPO−OH 3	179.4, 189.6[c]	DEPMPO−OH 3	183.8
DIPPMPO-1	330.8	DIPPMPO−OH 1	320.1	DIPPMPO−OH 1	321.6
DIPPMPO-2	82.2	DIPPMPO−OH 2	34.6	DIPPMPO−OH 2	47.6
DIPPMPO-3	187.1	DIPPMPO−OH 3	189.6[c]	DIPPMPO−OH 3	186.0
TFCOMPO	8.9	TFCOMPO−OH	220.2, 214.9[c], 3.1[d]	TFCOMPO−OH	217.3
MSMPO	69.9[a]	MSMPO−OH	57.5[a]	MSMPO−OH	62.3[a]
TFSMPO	55.5[a]	TFSMPO−OH	49.8[a]	TFSMPO−OH	53.4[a]
AMPO	99.4	AMPO−OH	97.5[e], 192.3[c]	AMPO−OH	98.8[e]
CPPO	35.6[b]	CPCOMPO−OH	195.6[c]	CPPO−OH	38.6[b]
CPCOMPO	169.3			CPCOMPO−OH	193.8

[a] Based on ∠***C***H_3-***C***−***S***−***C***. [b] ∠CH_2-***C***−***C***H_2-***C***H_2. [c] With intramolecular H-bonding O−H- - -O=C (or O−H- - -O=P). [d] *C*−*F*- - - -H−O. [e] *N*−*H*- - -O−N.

Table 4. Relative Total Energy (in kcal/mol) and Dipole Moment (in Debye) of the Theoretically Optimized Nitrone Structures at the B3LYP/6-31+G**//B3LYP/6-31G* Level

nitrone	rel *E*[a]	rel *H* (298 K)	dipole[b]
HMPO	n/a	n/a	4.03
DMPO	n/a	n/a	3.72
EMPO-1	0.0	0.0	4.56
EMPO-2	−0.2	−0.2	2.92
EMPO-3	0.2	0.3	2.83
BocMPO-1	0.0	0.0	4.34
BocMPO-2	0.5	0.6	2.39
DEPMPO-1	0.0	0.0	4.75
DEPMPO-2	1.9	1.8	1.16
DEPMPO-3	−2.2	−2.1	3.36
DIPPMPO-1	0.0	0.0	4.50
DIPPMPO-2	2.5	2.5	2.20
DIPPMPO-3	−1.8	−1.7	3.24

[a] Values are in kcal/mol relative to their respective conformer 1. [b] At B3LYP/6-31G(d) level.

D) and DMPO−OH (2.5 D) adducts (Table 5) are small compared to those of their respective nitrone forms (Table 4). The same trend is observed for the dipole moments of the most energetically favorable isomers of EMPO−OH (2.80 D) and BocMPO−OH (3.00 D) adducts compared to those of their respective stable nitrone conformations. However, the trend is reversed for DEPMPO−OH and DIPPMPO−OH adducts in which the dipole moments of the preferred conformations are more polar than those of their respective preferred nitrone conformations. This may indicate a more favorable formation of the •OH adduct for phosphorylated nitrones in aqueous media compared to DMPO and carboxylated nitrones.

VI. Reaction of OH Radical with Nitrones

Shown in Table 6 are thermodynamic data for the addition of •OH to a variety of nitrones. In general, all of these reactions are highly exoergic. Previously reported[37] ΔE_{rxn} for the reaction of H_2C=NHO with •OH was −58.27 kcal/mol at the MP2/6-31G(d) level of theory and is similar to that obtained at the B3LYP/6-31+G**//B3LYP/6-31G* level. The thermodynamic data are even more favorable as compared to •OH addition to monocyclic aromatic hydrocarbons at the same level of theory ΔE_{rxn} (298K) = 12−30 kcal/mol.[61] In general, reactions of alkoxycarbonyl nitrones with •OH are relatively less exoergic than •OH addition to alkoxyphosphoryl nitrones. Carboxylated nitrones have preference for formation of •OH adducts with the *trans*-1 configuration, while phosphorylated nitrones favor formation of the *cis*-3 isomer with intramolecular H-bonding. For reactions involving preferred conformational as well as configurational isomers for nitrones and their spin adducts, i.e., EMPO-2 to EMPO−OH *trans*-1; BocMPO-1 to BocMPO−OH *trans*-1; DEPMPO-3 to DEPMPO−OH *cis*-3 (with H-bond); DIPPMPO-3 to DIPPMPO−OH *cis*-3 (with H-bond), the overall reaction free energy was predicted to be most favorable in DIPPMPO followed by EMPO > BocMPO > DEPMPO > DMPO (in order of more positive values of ΔG_{rxn}). Moreover, values of ΔG_{rxn} follow a similar order for nitrones with less preferred conformations except for DEPMPO-1 or -2, which yielded more negative free energies than the alkoxycarbonyl nitrones.

B3LYP calculations suggest that transition-state structures do not exist for HMPO or DMPO as well as for the less exothermic reaction path for EMPO and DEPMPO. Potential energy surfaces are very similar for all of the representative nitrones.

Figure 5 shows the asymptotic profile of the addition channel (i.e., a barrierless process) for the addition of •OH to DMPO as well as for EMPO-2 and DEPMPO-1 to give EMPO−OH *cis*-2 and DEPMPO−OH *trans*-1, respectively. Changes in geometry on the nitronyl C and N are evident, i.e. from planar

(61) Barckholtz, C.; Barckholtz, T. A.; Hadad, C. M. *J. Phys. Chem. A* **2001**, *105*, 140−152.

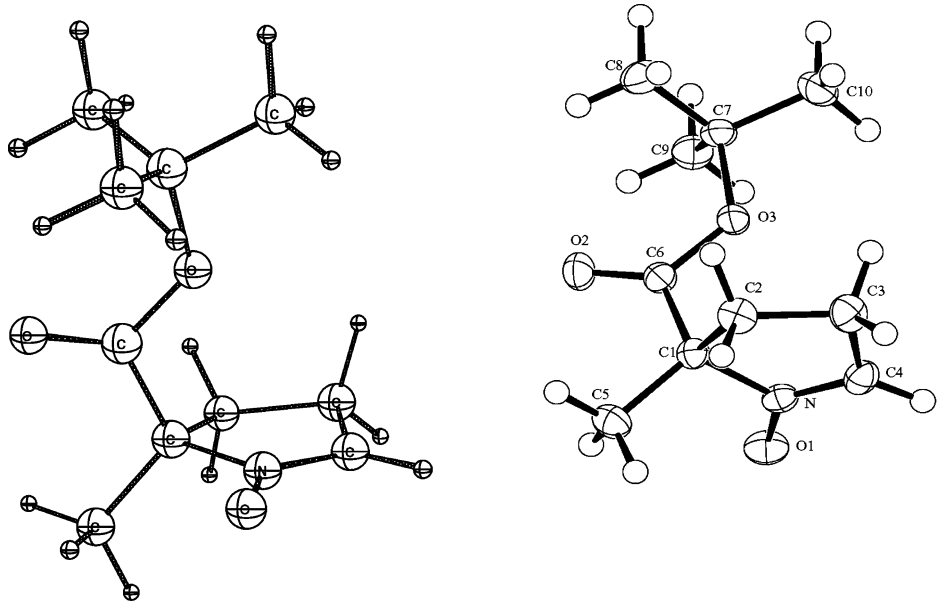

Figure 4. ORTEP view of X-ray structure of BocMPO (right). Displacement ellipsoids are drawn at 50% probability. Hydrogen atoms are represented as circles of arbitrary radius. Calculated structure at the B3LYP/6-31G* level is shown on the left.

Table 5. Relative Total Energy (E_{Tot} in kcal/mol) and Dipole Moment (in debye) of the Theoretically Optimized Spin Adduct Structures at the B3LYP/6-31+G**//B3LYP/6-31G* Level

spin adduct	rel E^a	rel H (298 K)	dipole[b]
OH radical	n/a	n/a	1.73
HMPO−OH	n/a	n/a	2.23
DMPO−OH	n/a	n/a	2.50
EMPO−OH *cis*-1	0.0	0.0	2.39
EMPO−OH *cis*-2	0.0	0.1	1.67
EMPO−OH *cis*-3[c]	−0.1	0.2	5.60
EMPO−OH *trans*-1	−0.9	−0.7	2.80
EMPO−OH *trans*-2	−0.6	−0.4	1.33
EMPO−OH *trans*-3	−0.5	−0.3	3.44
BocMPO−OH *cis*-1	0.0	0.0	2.44
BocMPO−OH *cis*-2	−0.2	−0.2	1.10
BocMPO−OH *cis*-3[c]	−0.4	−0.2	5.67
BocMPO−OH *trans*-1	−1.1	−0.9	3.00
BocMPO−OH *trans*-2	−0.9	−0.8	1.52
BocMPO−OH *trans*-3	−0.7	−0.6	3.66
DEPMPO−OH *cis*-1	0.0	0.0	3.55
DEPMPO−OH *cis*-2	−0.1	−0.1	1.16
DEPMPO−OH *cis*-3	−0.2	−0.3	2.89
DEPMPO−OH *cis*-3[c]	−3.6	−3.3	4.30
DEPMPO−OH *trans*-1	−0.2	0.0	3.59
DEPMPO−OH *trans*-2	−1.0	−0.9	1.88
DEPMPO−OH *trans*-3	−1.6	−1.6	2.24
DIPPMPO−OH *cis*-1	0.0	0.0	3.37
DIPPMPO−OH *cis*-2	−0.2	−0.2	0.72
DIPPMPO−OH *cis*-3[c]	−4.3	−4.1	4.10
DIPPMPO−OH *trans*-1	−0.4	−0.9	3.59
DIPPMPO−OH *trans*-2	−1.6	−1.5	1.74
DIPPMPO−OH *trans*-3	−2.3	−2.4	2.87

[a] Values are in kcal/mol relative to their respective isomer *cis*-1. [b] At B3LYP/6-31G(d) level. [c] With H-bonding.

to trigonal pyramidal for N, and planar to tetrahedral for C as the C−O distance is decreased. This barrierless process is consistent with that reported for •OH addition to $H_2C{=}NHO$.[37]

Our initial results on the kinetics of spin trapping of •OH[35] and $O_2^{\bullet-}$ [34] indicate that the rate of reaction is dependent on the charge of the nitronyl C based on semiempirical calculations. Current results based on DFT calculations parallel that of the semiempirical results we previously reported.[35] Table 7 shows the charge densities on the nitronyl C, the site of •OH addition. In general, charge densities on the nitronyl C of the most preferred conformations are most positive in DEPMPO-3 and DIPPMPO-3, 0.009 and 0.007, respectively, compared to BocMPO-1 (−0.006), EMPO-2 (−0.001), and DMPO (−0.022). Higher rate constants for the trapping of •OH by alkoxycarbonyl and alkoxyphosphoryl nitrones compared to DMPO could be accounted for the significantly high negative charge density on the nitronyl C of DMPO compared to the substituted nitrones, i.e., the k_{app} (M^{-1} s^{-1}) for trapping of •OH[35] are found to be: $1.93 \pm 0.05 \times 10^9$ for DMPO, $4.99 \pm 0.36 \times 10^9$ for EMPO, $4.48 \pm 0.32 \times 10^9$ for BocMPO, $4.83 \pm 0.34 \times 10^9$ for DEPMPO, and $4.59 \pm 0.22 \times 10^9$ DIPPMPO. Figure 7 shows the correlation of ΔG_{rxn} values with nitronyl C charge densities.

VII. Stability of Spin Adducts

Unimolecular decomposition of •OH adducts with a β-H could proceed via β-cleavage of the HC−N bond as shown in Scheme 3. A similar decomposition pathway was proposed for the 2-TFDMPO−OH adduct

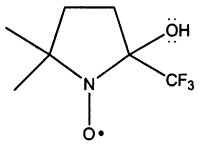

2-TFDMPO-OH

in which its higher stability compared to that of the DMPO−OH adduct was suggested to be due to a stronger C−N bond resulting from the electron-withdrawing inductive and field effects of the CF_3 substituent.[62] This mechanism for unimolecular decomposition is further supported by the shorter half-life of DMPO−OH adduct in basic media.[63] The C−N bond strength can therefore be influenced by charge on the nitroxyl N which in turn can be affected by the inductive effect from

(62) Janzen, E. G.; Zhang, Y.-K.; Arimura, M. *J. Org. Chem.* **1995**, *60*, 5434−5440.
(63) Marriott, P. R.; Perkins, M. J.; Griller, D. *Can. J. Chem.* **1980**, *58*, 803−807.

Table 6. Thermodynamic Parameters for the Reaction of Nitrones with OH Radical[a]

spin adducts	$E_{0,rxn}$	ΔH_{rxn}	ΔG_{rxn}	spin adducts	$E_{0,rxn}$	ΔH_{rxn}	ΔG_{rxn}
HMPO				DIPPMPO-1			
HMPO−OH	−60.96	−52.56	−42.58	*cis*-1	−50.68	−51.95	−41.22
DMPO				*cis*-2	−51.00	−52.15	−41.90
DMPO−OH	−50.70	−51.76	−42.07	*cis*-3[b]	−54.75	−56.08	−45.80
EMPO-1				*trans*-1	−51.51	−52.64	−42.47
cis-1	−51.57	−52.53	−43.61	*trans*-2	−52.18	−53.42	−42.83
cis-2	−51.46	−52.48	−42.91	*trans*-3	−53.24	−54.31	−44.42
cis-3[b]	−51.12	−52.35	−41.87	DIPPMPO-2			
trans-1	−52.25	−53.25	−44.04	*cis*-1	−53.09	−54.48	−42.30
trans-2	−51.91	−52.95	−43.45	*cis*-2	−53.41	−54.68	−42.98
trans-3	−51.85	−52.85	−43.72	*cis*-3[b]	−57.15	−58.60	−46.88
EMPO-2				*trans*-1	−53.91	−55.17	−43.55
cis-1	−51.32	−52.34	−42.90	*trans*-2	−54.58	−55.95	−43.91
cis-2	−51.21	−52.29	−42.20	*trans*-3	−55.65	−56.83	−45.50
cis-3[b]	−50.87	−52.16	−41.16	DIPPMPO-3			
trans-1	−52.00	−53.05	−43.34	*cis*-1	−49.02	−50.25	−39.83
trans-2	−51.66	−52.76	−42.74	*cis*-2	−49.34	−50.45	−40.50
trans-3	−51.60	52.66	−43.02	*cis*-3[b]	−53.09	−54.37	−44.40
EMPO-3				*trans*-1	−49.84	−50.94	−41.07
cis-1	−51.83	−52.78	−43.51	*trans*-2	−50.51	−51.72	−41.44
cis-2	−51.72	−52.73	−42.81	*trans*-3	−51.58	−52.61	−43.02
cis-3[b]	−51.38	−52.61	−41.78				
trans-1	−52.51	−53.50	−43.95	TFMPO			
trans-2	−52.17	−53.20	−43.35	*cis*	−51.76	−52.79	−43.22
trans-3	−52.11	−53.11	−43.63	*cis*[b]	−49.48	−50.57	−40.76
BocMPO-1				*trans*	−51.89	−52.93	−43.40
cis-1	−50.41	−51.51	−41.51	TFCOMPO			
cis-2	−50.61	−51.70	−41.88	*cis*	−50.28	−51.78	−41.54
cis-3[b]	−50.35	−51.67	−40.83	*cis*[c]	−50.36	−51.46	−40.50
trans-1	−51.37	−52.45	−42.82	*cis*[b]	−47.73	−48.93	−38.32
trans-2	−51.15	−52.28	−42.29	*trans*	−37.64	−53.12	−43.01
trans-3	−51.02	−52.08	−42.45	MSMPO			
BocMPO-2				*cis*	−67.77	−54.39	−44.53
cis-1	−51.02	−52.09	−41.96	*trans*	−69.75	−56.45	−46.78
cis-2	−51.22	−52.27	−42.33	TFSMPO			
cis-3[b]	−50.95	−52.25	−41.27	*cis*	−46.07	−55.52	−45.58
trans-1	−51.98	−53.03	−43.26	*trans*	−48.02	−56.97	−47.11
trans-2	−51.76	−52.86	−42.74	AMPO			
trans-3	−51.63	−52.66	−42.89	*cis*	−52.20	−50.94	−41.12
DEPMPO-1				*cis*[c]	−47.96	−46.02	−35.73
cis-1	−51.73	−52.89	−42.60	*trans*[d]	−26.56	−50.94	−41.41
cis-2	−51.90	−52.96	−43.56	CPCOMPO			
cis-3	−52.15	−53.17	−43.96	*cis*[c]	−159.83	−51.94	−41.19
cis-3[b]	−54.81	−56.16	−45.53	*trans*	−160.57	−52.86	−43.01
trans-1	−51.73	−52.88	−42.83	CPPO			
trans-2	−52.77	−53.81	−44.63	CPPO−OH	−186.00	−52.13	−42.27
trans-3	−53.44	−54.48	−45.41				
DEPMPO-2				DMMPO-2			
cis-1	−53.38	−54.73	−42.58	*cisA*	−43.40	−44.37	−34.39
cis-2	−53.55	−54.80	−43.54	*cisB*	−46.70	−47.68	−38.15
cis-3	−53.79	−55.02	−43.94	DMMPO-3			
cis-3[b]	−56.45	−58.00	−45.51	*cis*	−48.07	−49.32	−38.64
trans-1	−53.37	−54.73	−42.81	*trans*	−49.59	−50.60	−41.18
trans-2	−54.41	−55.66	−44.61	DMMPO-4			
trans-3	−55.08	−56.32	−45.39	*cis*	−48.63	−49.57	−39.58
DEPMPO-3				*trans*	−51.86	−52.95	−42.51
cis-1	−49.47	−50.75	−39.56	DMMPO-5			
cis-2	−49.64	−50.82	−40.52	*cis*	−52.21	−53.36	−43.26
cis-3	−49.88	−51.04	−40.93	*trans*	−51.59	−52.57	−42.49
cis-3[b]	−52.54	−54.02	−42.50				
trans-1	−49.46	−50.75	−39.80				
trans-2	−50.50	−51.68	−41.59				
trans-3	−51.17	−52.34	−42.38				

[a] B3LYP/6-31+G**//B3LYP/6-31G* reaction (rxn) energies are reported relative to reactants, in kcal/mol. $E_{0,rxn}$ energies include scaled ZPE. ΔH_{rxn} and ΔG_{rxn} are given at 298.15 K.

the substituent at the C-5 position. It is assumed that a relatively negative charge density on the N can stabilize the C−N. As shown in Table 8, substituents have little effect on the charge density of C-2, β-H, and O, while charges on C-5 and N are quite varied, depending on the nature of the substituents. Therefore, it is hypothesized that one of the factors that could

Table 7. Charge Densities on C-2 of the Theoretically Optimized Nitrones Structures at the B3LYP/6-31+G**//B3LYP/6-31G* Level

nitrone	charge density	nitrone	charge density
HMPO	0.104	DIPPMPO-3	0.007
DMPO	−0.022	TFMPO	−0.003
EMPO-1	−0.005	TFCOMPO	0.000
EMPO-2	−0.001	MSMPO	0.009
EMPO-3	−0.000	TFSMPO	0.011
BocMPO-1	−0.006	AMPO	0.025
BocMPO-2	−0.003	CPPO	−0.017
DEPMPO-1	−0.005	CPCOMPO	0.007
DEPMPO-2	−0.011	DMMPO-5	−0.001
DEPMPO-3	0.009	DMMPO-4	−0.030
DIPPMPO-1	−0.006	DMMPO-3	−0.051
DIPPMPO-2	−0.020	DMMPO-2	−0.232

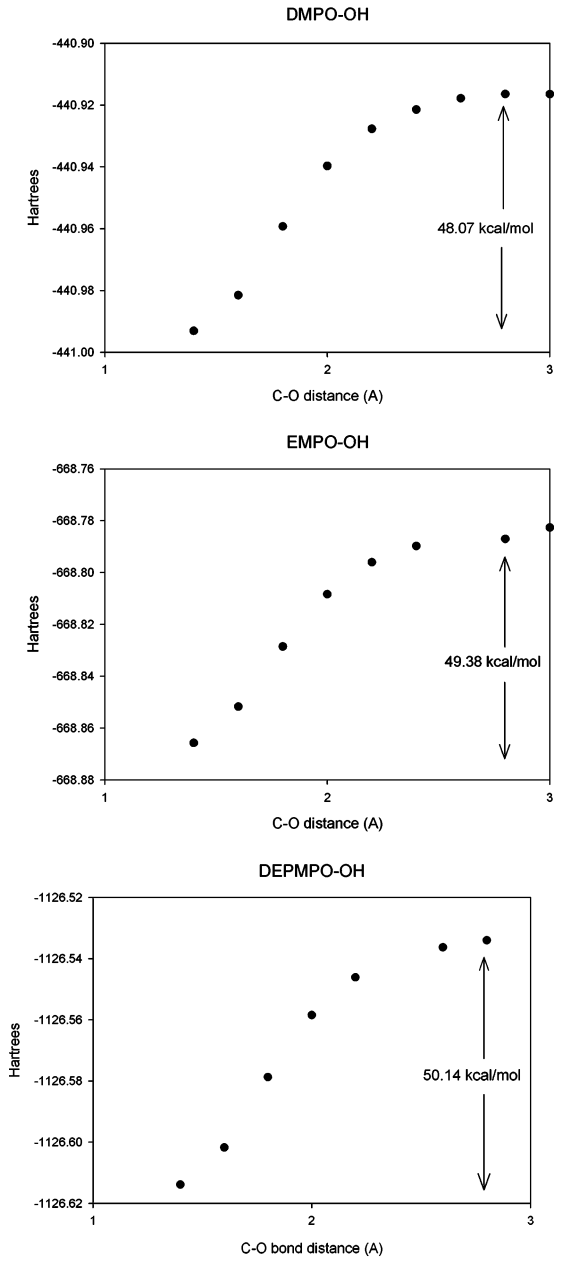

Figure 5. Asymptotic reaction profile for the addition of •OH with nitrones DMPO, EMPO, and DEPMPO. Each data point corresponds to a fully optimized geometry and energy with the C−O distance constrained at the indicated value.

influence unimolecular decomposition of nitroxides bearing β-H are the charge densities around the nitroxyl moiety. A qualitative

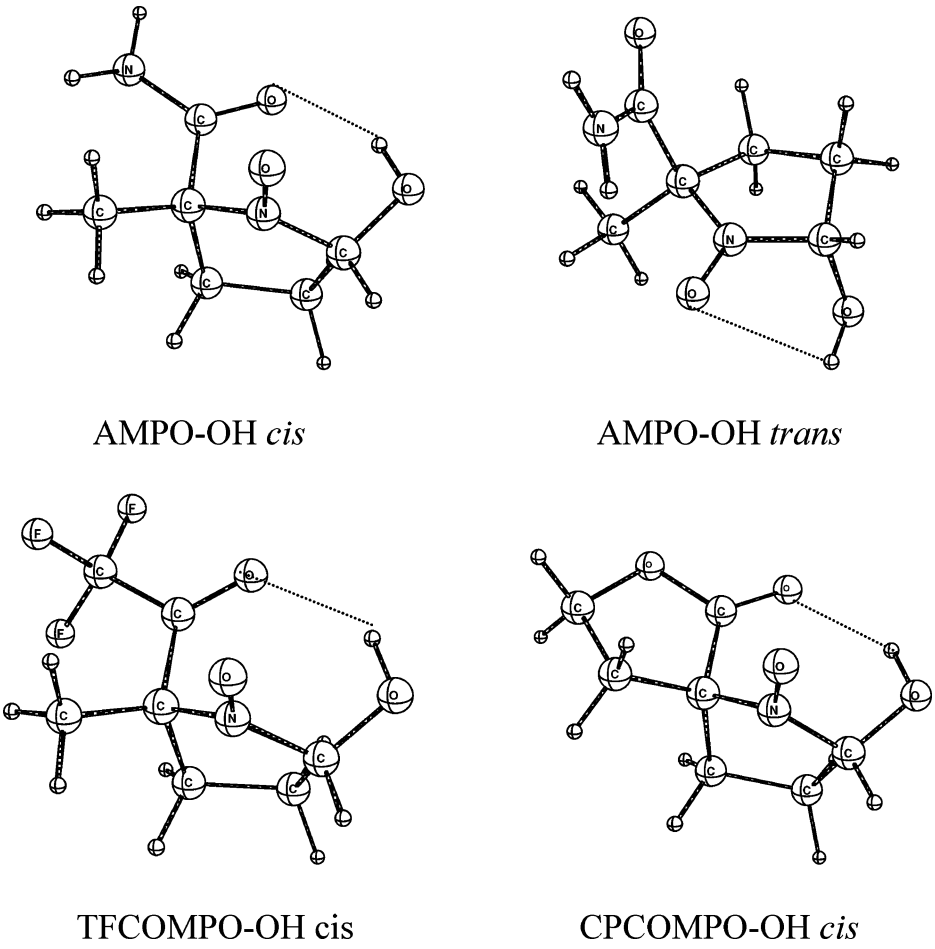

Figure 6. Hydroxyl radical adducts exhibiting intramolecular H-bonding in optimized structures of hypothetical spin traps at the B3LYP/6-31G* level of theory. Broken lines indicate sites of intramolecular H-bonding and their distances are shown in Table 2.

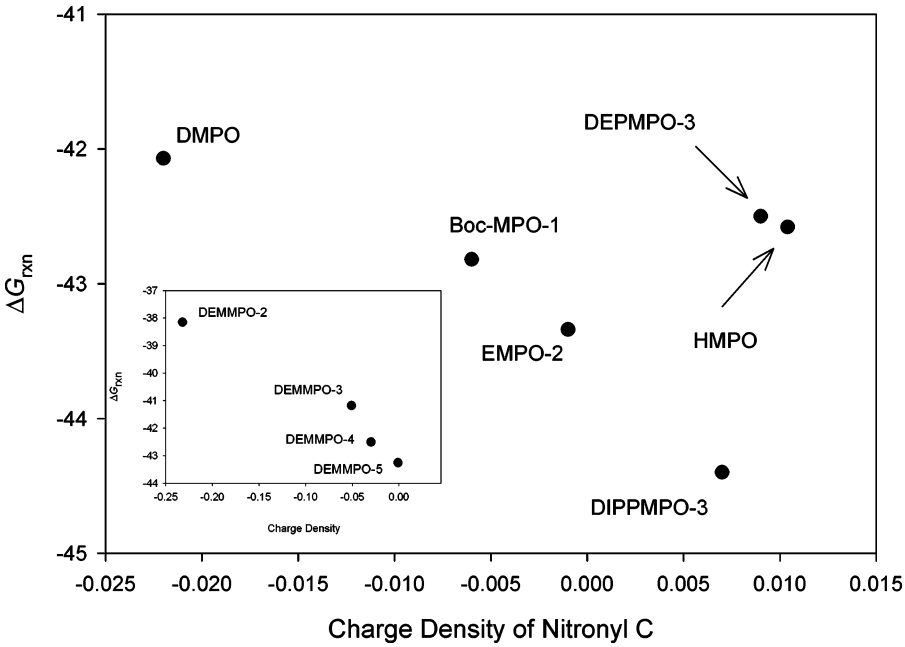

Figure 7. Plot of charge densities of nitronyl C of the most favored conformation of various substituted nitrones versus reaction free energies (ΔG_{rxn}) for the formation of their respective most stable •OH adduct isomer. Inset: For DEMMPO analogues.

comparison of the calculated charge densities on the nitroxyl N, C-5, and the C-2 of the most stable spin adducts (i.e., *trans*-1 isomers of EMPO−OH and BocMPO−OH, and the H-bonded *cis*-3 isomers of DEPMPO−OH and DIPPMPO−OH) including DMPO−OH showed no significant difference among the charges on C-2 except for the less negative charge on the nitroxyl N and more positive charge on the C-5 in alkoxycarbonyl nitroxides compared to alkoxyphosphoryl •OH adducts.

Scheme 3

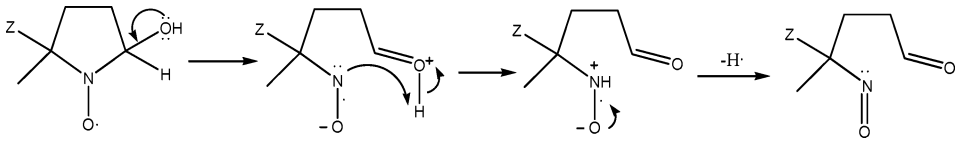

The electronic characteristics of these adducts are consistent with their reported stability[35] since the N−C bond-breaking process should be more facile when the nitroxyl N is less negative. Also, the charge density on N for alkoxycarbonyl nitroxides with H-bonding is relatively more negative compared to the charge densities for those adducts without H-bonding. Interestingly, the charge on C-5 for DMPO−OH is most positive (0.082) compared to the rest of the substituted adducts but with N charge of (−0.022) which is higher than those of alkoxycarbonyl nitroxides (∼−0.01) but lower than those of the phosphorylated adducts (∼−0.03). This may explain why DMPO−OH adduct has a shorter half-life relative to the substituted •OH adducts, since a positively charged C-5 could facilitate a favorable HC−N bond-breaking process as was depicted in Scheme 3. The charge on N for adducts exhibiting intramolecular H-bonding is relatively more negative compared to that for other adducts without such H-bonding. Figure 8 shows an approximate correlation of the charge densities of nitronyl N with various half-lives of the •OH adducts.

Bimolecular decomposition of •OH adducts has been reported[64] to produce diamagnetic species as secondary decomposition products of the hydroxylamine and nitrone (Scheme 4). The ease of β-H abstraction from the •OH adduct was postulated to be dependent on the conformation of the β-H relative to the singly occupied orbital on the nitroxyl nitrogen.[65] Further support of H-abstraction as the major cause of decomposition is the short half-lives of •OH adducts in basic media.[66] A low activation energy for this reaction occurs when the singly occupied orbital is in the same plane as the H atom to be abstracted. This corresponds to a dihedral $\angle O-N-C-H$ close to 90°. It is predicted that the low dihedral $\angle O-N-C-H$ of the preferred isomers DEPMPO−OH *cis*-3 (59.5°) and DIPPMPO−OH *cis 3* (46°) (Table 8) with strong H-bonding will have longer half-lives compared to the alkoxycarbonyl nitrones, EMPO and BocMPO as well as DMPO. Our recent experimental results[35] indicate that DEPMPO and DIPPMPO have significantly longer pseudo-first-order half-lives of about 130−158 min as compared to 55 min for DMPO and BocMPO (with the exception of EMPO with $t_{1/2}$ of about 127 min). Figure 8 shows an approximate correlation of the $\angle O-N-C-H$'s with various half-lives of the •OH adducts. Moreover, the unpaired electron is almost equally distributed between the N−O bond with an average of 52% localization on O for all preferred isomers.

VIII. Other Functional Groups as Substituents

Electronic and thermodynamic properties of novel nitrones containing electron-withdrawing substituents (Scheme 5), such as $-CF_3$, $-COCF_3$, $-SO_2Me$, $-SO_2CF_3$, and $-CONH_2$, were compared and are shown in Table 9. Alkyl and spirocarbonyl nitrones were also used as models. Although only one conformational isomer for each of the nitrones was considered, we explored two possible isomers for each of the spin adducts, i.e., *cis* and *trans* configurations. We also compared the electronic properties and energetics of the *cis* isomers with and without intramolecular H-bonding, since alkoxyphosphoryl nitrones demonstrated that this aspect is crucial, at least for thermodynamic favorability of •OH addition to nitrones. Intramolecular H-bonding (Table 2) between N−H and N−O was predicted in AMPO−OH *trans* with a N−H---O−N bond distance of 2.09 Å (Figure 6). However, intramolecular H-bonding was not observed in some spin adducts bearing a sulfonyl (MSMPO−OH *cis* and TFSMPO−OH *cis*) group. Contrary to the observation made in alkoxyphosphoryl nitrone •OH adducts, conformations of all of the •OH adducts exhibiting H-bonding are not energetically preferred (Table 9). In most cases, the *trans* •OH adduct is the preferred configuration. Trifluoromethyl nitrone (TFMPO) and amido nitrone (AMPO) showed no significant energy preference for either the *cis* and *trans* isomers for their •OH adduct, with relative energies of only 0.1 and 0.0 kcal/mol, respectively. In the case of AMPO−OH, the isomeric form either *cis* or *trans* with N−H····O−N intramolecular H-bonding are more preferred than *cis* isomers having intramolecular H-bonding between the carbonyl O and the hydroxyl H.

In all cases, reaction free energies (Table 6) also indicate that formation of the *trans* isomers are more thermodynamically favored than the *cis* isomers and even more favorable than the *cis* isomer with an intramolecular H-bond. These energy differences show that formation of the *trans* isomer is favored by ca. 1−2 kcal/mol relative to the *cis* isomer. For TFMPO and AMPO this free-energy difference, however, is only ca. 0.2−0.3 kcal/mol. Reaction free energies range from −41.41 to −47.11 kcal/mol and are highest for the formation of spin adducts from MSMPO and TFSMPO with ΔG_{rxn} of −46.78 and −47.11 kcal/mol, respectively.

Since none of the molecules mentioned in this section have been synthesized or reported to trap •OH (except for CPPO),[67] we therefore could not do any correlations with experimental kinetic data. We can, however, make predictions as to the possible spin-trapping characteristics of these hypothetical molecules based on the structure−reactivity correlation made previously for DMPO, alkoxycarbonyl, and alkoxyphosphoryl nitrones. Charge densities on nitronyl C of sulfonylated-nitrones (MSMPO and TFSMPO), AMPO, and spirocarbonyl nitrone CPCOMPO are significantly more positive than other substituted nitrones (Table 7). These charge densities are comparable in magnitude to those of DEPMPO (0.009) and DIPPMPO (0.007), with values ranging from 0.007 to 0.025, with amido nitrone AMPO having the greatest positive charge. Surprisingly, the

(64) Khramtsov, V.; Berliner, L. J.; Clanton, T. L. *Magn. Reson. Med.* **1999**, *42*, 228−234.
(65) Breuer, E.; Aurich, H. G.; Nielsen, A. *Nitrones, Nitronates and Nitroxides*; John Wiley and Sons: New York, 1989.
(66) Rosen, G. M.; Britigan, B. E.; Halpern, H. J.; Pou, S. *Free Radicals: Biology and Detection by Spin Trapping*; Oxford Univeristy Press: New York, 1999.
(67) Turner, M. J.; Rosen, G. M. *J. Med. Chem.* **1986**, *29*, 2439−2444.

Table 8. Dihedral Angles and Charge Densities of the Theoretically Optimized •OH Adduct Structures at the B3LYP/6-31+G**//B3LYP/6-31G* Level

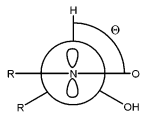

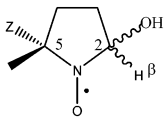

Spin Adduct	*D(O-N-C-H)*	*Charge Density*				
	Θ	*N*	*C-5*	*C-2*	*β-H*	*O*
HMPO-OH	56.64	-0.024	-0.296	0.224	0.232	-0.420
DMPO-OH	63.92	-0.022	0.082	0.225	0.232	-0.424
EMPO-OH *cis-1*	83.24	-0.010	0.011	0.238	0.221	-0.422
EMPO-OH *cis-2*	72.87	-0.018	0.012	0.232	0.223	-0.406
EMPO-OH *cis-3*[a]	63.82	-0.033	0.009	0.228	0.247	-0.377
EMPO-OH *trans-1*	59.50	-0.012	0.009	0.229	0.234	-0.414
EMPO-OH *trans-2*	64.03	-0.019	0.012	0.227	0.233	-0.403
EMPO-OH *trans-3*	63.31	-0.008	0.011	0.229	0.237	-0.467
BocMPO-OH *cis-1*	83.74	-0.008	0.010	0.237	0.222	-0.425
BocMPO-OH *cis-2*	70.30	-0.018	0.011	0.229	0.224	-0.405
BocMPOH *cis-3*[a]	63.48	-0.031	0.008	0.228	0.246	-0.379
BocMPO-OH *trans-1*	58.33	-0.010	0.008	0.228	0.233	-0.416
BocMPO-OH *trans-2*	63.33	-0.018	0.012	0.227	0.232	-0.406
BocMPO-OH *trans-3*	63.63	-0.007	0.010	0.230	0.236	-0.413
DEPMPO-OH *cis-1*	79.68	-0.026	-0.260	0.236	0.222	-0.420
DEPMPO-OH *cis-2*	69.23	-0.020	-0.265	0.236	0.221	-0.425
DEPMPO-OH *cis-3*[a]	59.48	-0.036	-0.270	0.227	0.249	-0.396
DEPMPO-OH *cis-3*	78.57	-0.020	-0.267	0.239	0.218	-0.434
DEPMPO-OH *trans-1*	55.27	-0.030	-0.260	0.229	0.230	-0.410
DEPMPO-OH *trans-2*	60.93	-0.021	-0.273	0.229	0.234	-0.419
DEPMPO-OH *trans-3*	66.39	-0.025	-0.268	0.231	0.236	-0.421
DIPPMPO-OH *cis-1*	82.71	-0.023	-0.261	0.239	0.220	-0.424
DIPPMPO-OH *cis-2*	66.23	-0.022	-0.267	0.235	0.221	-0.422
DIPPMPO-OH *cis-3*[a]	46.00	-0.032	-0.279	0.229	0.252	-0.401
DIPPMPO-OH *trans-1*	55.08	-0.030	-0.260	0.229	0.232	-0.410
DIPPMPO-OH *trans-2*	64.30	-0.021	-0.273	0.229	0.234	-0.419
DIPPMPO-OH *trans-3*	81.65	-0.025	-0.268	0.231	0.236	-0.437
TFMPO-OH *cis*	70.67	-0.028	0.012	0.236	0.222	-0.396
TFMPO-OH *cis*[a]	58.53	-0.046	0.010	0.228	0.250	-0.362
TFMPO-OH *trans*	63.79	-0.023	0.009	0.238	0.227	-0.402
TFCOMPO-OH *cis*	78.09	-0.019	0.010	0.238	0.222	-0.401
TFCOMPO-OH *cis*[a]	65.32	-0.036	0.007	0.229	0.250	-0.367
TFCOMPO-OH *cis*[b]	67.02	-0.038	0.008	0.234	0.245	-0.373
TFCOMPO-OH *trans*	61.84	-0.015	0.009	0.229	0.240	-0.398
MSMPO-OH *cis*	66.32	-0.047	-0.077	0.241	0.221	-0.378
MSMPO-OH *trans*	65.85	-0.045	-0.078	0.233	0.242	-0.376
TFSMPO-OH *cis*	64.17	-0.052	-0.051	0.238	0.227	-0.361
TFSMPO-OH *trans*	64.25	-0.053	-0.055	0.232	0.243	-0.360
AMPO-OH *cis*	79.90	-0.006	0.018	0.234	0.224	-0.453
AMPO-OH *cis*[a]	61.33	-0.031	0.016	0.227	0.248	-0.382
AMPO-OH *trans*	47.91	-0.012	0.019	0.227	0.234	-0.441
CPPO-OH	52.41	-0.011	0.088	0.226	0.231	-0.425
CPCOMPO-OH *cis*	60.68	-0.026	-0.010	0.226	0.251	-0.372
CPCOMPO-OH *trans*	60.51	-0.005	-0.006	0.229	0.240	-0.407
DMMPO-5-OH *cis*	60.18	-0.043	-0.469	0.225	0.249	-0.371
DMMPO-5-OH *trans*	44.61	-0.033	-0.468	0.225	0.258	-0.391
DMMPO-4-OH *cis*	65.84	-0.040	-0.290	0.233	0.240	-0.388
DMMPO-4-OH *trans*	65.85	-0.021	-0.292	0.226	0.236	-0.413
DMMPO-3-OH *cis*	62.75	-0.036	-0.296	0.232	0.249	-0.387
DMMPO-3-OH *trans*	67.61	-0.017	-0.300	0.230	0.242	-0.419
DMMPO-2-OH[d]	n/a	-0.030	-0.293	0.053	n/a	-0.392
DMMPO-2-OH[e]	n/a	-0.026	-0.291	0.043	n/a	-0.393

[a] *C═O*- - -O−H or P═O- - -O−H. [b] *C−F*- - -H−O. [c] *N−H*- - -O−N. [d] Conformer-3. [e] Conformer-1.

spirocarbonyl nitrone CPCOMPO also gave a positive charge density of 0.007 on the nitronyl C, contrary to the observed charge densities found in the other carbonylated nitrones EMPO (−0.001 to −0.005) and BocMPO (−0.003 to −0.006) and the alkylspiro nitrone analogue CPPO (−0.017). These results indicate that a combination of bond constraints and presence

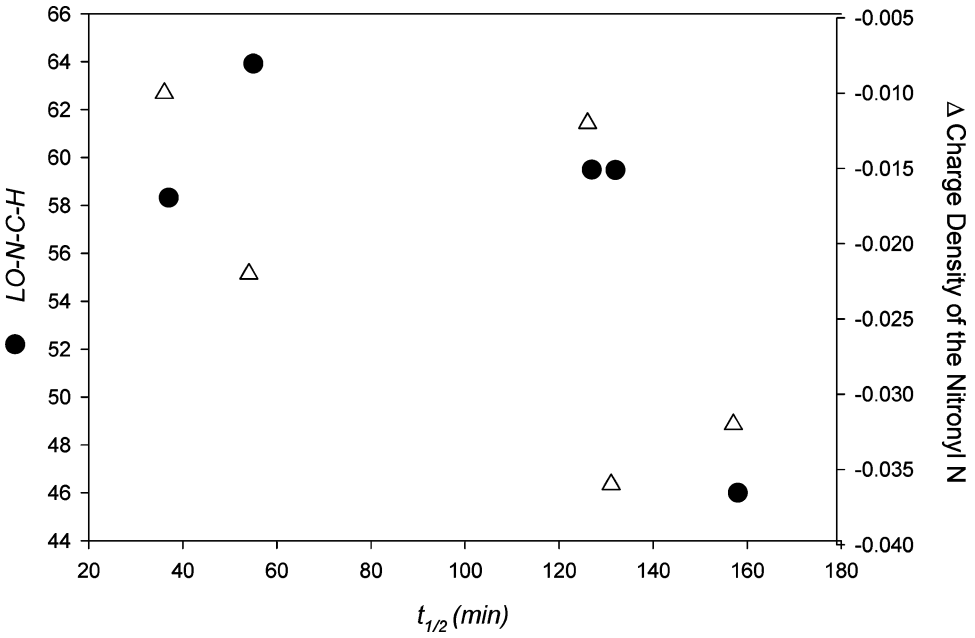

Figure 8. Plots of $\angle O-N-C-H$ (•) and nitroxyl N (Δ) of the most favored •OH adducts of DMPO, EMPO, BocMPO, DEPMPO, DIPPMPO versus their respective experimental half-lives.

Scheme 4

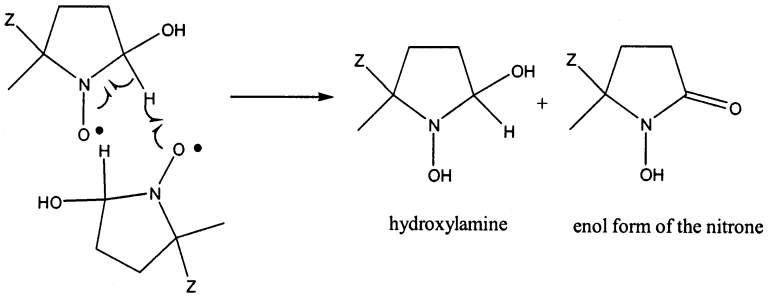

Scheme 5

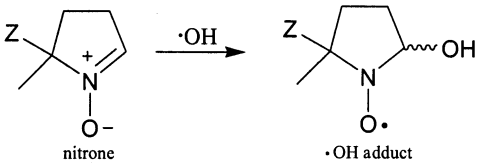

nitrone	Z
TFMPO	$-CF_3$
TFCOMPO	$-COCF_3$
MSMPO	$-SO_2Me$
TFSMPO	$-SO_2CF_3$
AMPO	$-CONH_2$
CPPO	$-CH_2CH_2CH_2CH_2^-$
CPCOMPO	$-C(O)OCH_2CH_2^-$

of a carbonyl group could significantly affect the charge density on the nitronyl C.

The dihedral $\angle O-N-C-H$ is smallest in AMPO−OH *trans* (47.9°), which is essentially the same as that of DIPPMPO−OH *cis*-3 (46.0°), which is the most preferred spin adduct isomer and the most long-lived •OH adduct (Table 8). The spiro nitrones CPPO−OH (52.4°) and CPCOMPO−OH (60.5°), and TFCOMPO (61.8°) are other *trans* •OH adducts that exhibit small $\angle O-N-C-H$. Charge density values (Table 8) for almost all of the spin adducts are somewhat similar to those of the alkoxycarbonylated spin adducts with the exception of the sulfonylated adducts, MSMPO−OH and TFSMPO−OH, and CPCOMPO−OH which has negatively charged C-5 similar to those of the alkoxyphosphorylated adducts.

Although these calculations show that •OH addition to sulfonylated nitrones is the most thermodynamically favored compared to that in other substitutents, they may not be suitable for spin trapping since sulfonyl groups are known to react with •OH to form C-centered radicals.[68] It is predicted that AMPO and CPCPMPO may be good in spin trapping charged radicals such as $O_2^{\bullet-}$ and can form stable •OH adducts comparable to those of alkoxyphosphorylated nitrones. Although CPPO has less positive nitronyl C, it may be able to form stable •OH adducts based on its small dihedral $\angle O-N-C-H$ of 52.4°.

IX. Effect of Alkoxyphosphoryl Position

Alkoxyphosphosphoryl nitrones are one of the most studied spin traps due to their ability to form persistent $O_2^{\bullet-}$ and •OH

(68) Carton, P. M.; Gilbert, B. C.; Laue, H. A. H.; Norman, R. O. C.; Sealy, R. C. *J. Chem. Soc., Perkin Trans. 2* **1975**, *11*, 1245−1249.
(69) Roubaud, V.; Siri, D.; Tordo, P.; Hdii, F.; Reboul, J.-P. *Acta Crystallogr., Sect. C* **1998**, 825−827.
(70) Lide, D. R., Ed. *Handbook of Chemistry and Physics*, 50th ed.; CRC Press: Cleveland, 1969.
(71) Chaloner, P. A.; Harrison, R. M.; Hotchcock, P. B.; Pedersen, R. T. *Acta Crystallogr.* **1992**, *C48*, 717−720.
(72) Bats, J. W.; Weyrauch, J. P.; Hashmi, S. K. *Acta Crystallogr.* **2002**, *E58*, o590-o591.
(73) Hossain, M. B.; Van der Helm, D. *Acta Crystallogr.* **1983**, *C39*, 1297−1300.
(74) Dickman, M. H. *Acta Crystallogr.* **2001**, *E57*, o636−0637.

Table 9. Relative Total Energy (E_{tot} in kcal/mol) and Dipole Moment (in debye) of the Theoretically Optimized Structures at the B3LYP/6-31+G**//B3LYP/6-31G* Level

	rel E[a]	rel H (298 K)	dipole[e]
	Nitrone		
TFMPO	n/a	n/a	4.12
TFCOMPO	n/a	n/a	5.20
MSMPO	n/a	n/a	6.94
TFSMPO	n/a	n/a	5.69
AMPO	n/a	n/a	1.91
CPPO	n/a	n/a	3.66
CPCOMPO	n/a	n/a	5.19
	OH Adduct		
TFMPO *cis*	0.0	0.0	3.36
TFMPO *cis*[b]	2.2	2.2	3.95
TFMPO *trans*	−0.1	−0.1	2.76
TFCOMPO *cis*	0.0	0.0	3.94
TFCOMPO *cis*[c]	0.1	0.3	4.37
TFCOMPO *cis*[b]	2.8	2.9	4.06
TFCOMPO *trans*	−1.5	−1.3	2.53
MSMPO *cis*	0.0	0.0	6.21
MSMPO *trans*	−2.1	−2.1	5.07
TFSMPO *cis*	0.0	0.0	5.32
TFSMPO *trans*	−1.6	−1.5	4.00
AMPO *cis*[d]	0.0	0.0	1.83
AMPO *cis*[c]	4.7	4.9	5.88
AMPO *trans*[d]	−0.1	0.0	1.56
CPPO−OH	n/a	n/a	2.21
CPCOMPO *cis*[c]	0.0	0.0	5.91
CPCOMPO *trans*	−0.7	−0.9	3.78

[a] Values are in kcal/mol relative to their respective isomer *cis* isomers without H-bonding. H-bonding correspond to [b] *C−F- - -H−O*. [c] *C═O- - -O−H*. [d] *N−H- - -O−N*. [e] At B3LYP/6-31G(d) level.

Scheme 6

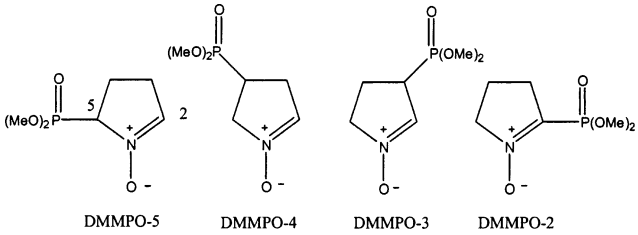

adducts compared to that of DMPO.[34,35] It is therefore worth examining the effect of the substituent position on the electronic and thermodynamic properties of these nitrones. By exploring the energetics of the four different positional isomers of dimethoxyphosphosphoryl nitrones (Scheme 6), it might be possible to predict the most efficient site of substitution for trapping •OH and the spin adduct stability based on their optimally calculated electronic and thermodynamic parameters. This work will only focus on the isomeric forms that are known to be favored in DEPMPO and DIPPMPO reactions with •OH, i.e., similar to that of the *cis*-3 conformer. Optimizations were performed starting with initial structures in which the P═O moiety is pointing toward the ring system.

Interestingly, DMMPO-2 is the most favored nitrone isomer, while DMMPO−OH *cis*-5 is the most favored isomer for the •OH adduct (Table 10). For C-3 and C-4 substituted nitrones, *trans* isomers are energetically more favored, while the *cis* configuration is more preferred at the C-5 position (Table 10). Formation of spin adducts from C-4- and C-5-substituted nitrones are more exothermic than from those for C-2- and C-3-substituted nitrones, and the formation of the DMMPO−OH *cis*-5 adduct is calculated to be the most exothermic. The DMMPO−OH *cis*-5 isomer exhibits strong intramolecular

Table 10. Relative Total Energy (in kcal/mol) and Dipole Moment (in debye) of the Theoretically Optimized Structures at the B3LYP/6-31+G**//B3LYP/6-31G* Level

compounds	rel E[a]	rel H (298 K)	dipole[d]
	Nitrones		
DMMPO-5	0.0	0.0	4.89
DMMPO-4	−3.4	−3.4	5.43
DMMPO-3	−4.0	−3.9	4.10
DMMPO-2	−5.1	−4.7	3.78
	OH Adduct		
DMMPO-5-OH *cis*	0.0	0.0	5.38
DMMPO-5-OH *trans*	0.9	0.8	3.73
DMMPO-4 OH *cis*	0.6	0.4	5.08
DMMPO-4 OH *trans*	−3.0	−3.0	3.35
DMMPO-3 OH *cis*	0.0	0.1	5.36
DMMPO-3 OH *trans*	−1.1	−1.1	3.69
DMMPO-2 OH *cis*[b]	4.9	4.3	2.98
DMMPO-2 OH *cis*[c]	1.4	1.0	4.22

[a] Values are in kcal/mol relative to DMMPO-5 for the nitrones and DMMPO−OH *cis* for the •OH adducts. [b] Conformer-3. [c] Conformer-1. [d] At B3LYP/6-31G(d) level.

Scheme 7

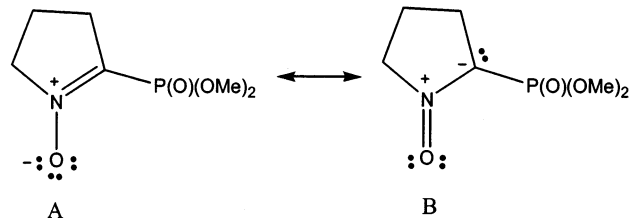

H-bonding of about 1.95 Å (Table 2), similar to those observed for DIPPMPO−OH *cis*-3 and DEPMPO−OH *cis*-3 isomers. This intramolecular H-bonding could be a major contributing factor in the stability of the molecule and its energetically favorable formation over its *trans* isomer. The DMMPO−OH *cis*-3 isomer with a much weaker H-bond of 2.08 Å is energetically less preferred than its *trans* counterpart. The coupled cluster method (CCSD) was performed on the DMMPO−OH *cis*-3 adducts with and without intramolecular H-bonding to demonstrate the validity of the B3LYP calculations. Results show a relative energy difference of less than 0.1 kcal/mol using CCSD/6-31+G**//B3LYP/6-31G* compared to that using the B3LYP/6-31+G**//B3LYP/6-31G* level (see Supporting Information Table 8).

The order of increasing positive charge on the nitronyl C is as follows: DMMPO-2 (−0.232) < DMMPO-3 (−0.051) < DMMPO-4 (−0.030) < DMMPO-5 (−0.001) (Table 7). This order predicts that substitution at the C-5 position makes the nitronyl C more reactive toward nucleophilic radicals, compared to the C-2 isomer (see inset of Figure 7). Close examination of the charge densities for the nitronyl N and O as well as for P upon going from position C-5 to C-2 reveals that the charge on N becomes more positive by 0.03, O is more negative in DMMPO-5 (by 0.05), and there is no significant perturbation on the charge for P. The large negative charge on the nitronyl C in DMMPO-2 is indicative of major resonance contribution from structure B (Scheme 7). This result predicts that phosphoryl substitution on C-2 may not be suitable for spin trapping of nucleophilic radicals such as O-centered ROS.

The $\angle O-N-C-H$ is lowest in DMMPO−OH *cis*-5 (60.2°) and DMMPO−OH *trans*-5 (44.6°) (Table 8). Although reaction enthalpies and free energies for the formation of both isomers do not differ significantly, we could expect that decay property

of the spin adducts will differ. On the basis of the dipole moments shown in Table 10, the following order of increasing polarity is predicted: DMMPO-2 (3.78 D) < DMMPO-3 (4.10 (D) < DMMPO-5 (4.89 D) < DMMPO-4 (5.43 D). In general, the *cis* configuration for the •OH adducts are more polar than their *trans* isomers.

X. Conclusions

Calculations of the minimum energy geometries of the commonly used nitrones as well as hypothetical ones, and their respective •OH spin adducts have been performed using density functional theory. The charge densities on nitronyl C and O were also calculated and used as a basis for the kinetic addition of hydroxyl radical and spin adduct decay. A barrierless energy path has been calculated for DMPO, EMPO, and DEPMPO−OH adduct formations, consistent with the large exoergicity of these addition reactions. Alkoxycarbonyl nitrones have a preference for formation of *trans* •OH adducts, while alkoxyphosphoryl nitrones favor the *cis* isomers with intramolecular H-bonding. Charge densities on nitronyl C, the site of •OH addition, are most positive for the most stable conformations of alkoxyphosphorylated nitrones compared to those of alkoxycarbonyl nitrones and DMPO, consistent with observed kinetic data for trapping •OH and $O_2^{\bullet-}$ radicals. Dihedral angles of the β-H relative to the singly occupied orbital of the nitroxide showed to be smallest in the *cis* adducts having intramolecular H-bonding in the alkoxyphosphorylated •OH adducts. This is also consistent with the relatively longer half-lives of alkoxyphosphorylated •OH adducts compared to alkoxycarbonyl •OH adducts and DMPO−OH.

Addition of •OH to sulfonylated nitrones is predicted to be the most thermodynamically favored reaction compared to other substituted nitrones; however, experimental evidence shows that sulfonyl groups are susceptible to •OH attack. Amido nitrone AMPO and spirocarbonyl nitrones CPCOMPO are predicted to exhibit high reactivity toward nucleophilic radicals and relatively persistent spin adducts, due to the high positive charge on the nitroxyl C and low dihedral $\angle O-N-C-H$, respectively. Moreover, although CPPO has a less positive nitronyl C, it may be able to form a stable •OH adduct as well.

Alkoxyphosphoryl group $-P(O)(MeO)_2$ substitution on C-2 is the most stable isomer, although its reactivity toward •OH is not thermodynamically preferred. Reaction enthalpies and free energy are highest for the formation of *cis* •OH adducts with $-P(O)(MeO)_2$ substitution on C-5. In addition, from a kinetic point of view, substitution at C-5 could provide an efficient spin trap for O-centered radicals with a long half-life for the spin adduct comparable to that of DIPPMPO−OH adducts.

This study demonstrates how theoretical analysis can be used as a tool to understand spin-trapping behavior of certain classes of nitrones and should be useful in designing better and more efficient spin traps for future applications. Experimental verification of these predictions will be reported in due course.

Acknowledgment. We thank the Ohio Supercomputer Center (OSC) for support of this research and Barbara Woodall of OSC for her assistance. To Prof. DeLanson R. Crist of the Chemistry Department Georgetown University for valuable suggestions. This work was supported by NIH Grants HL38324, HL63744, and HL65608. C.M.H. acknowledges support from the Ohio State Environmental Molecular Science Institute funded by the NSF.

Supporting Information Available: Energies, enthalpies, and free energies for all spin traps and their corresponding •OH adducts (PDF). X-ray cystallographic data (CIF). This material is available free of charge via the Internet at http://pubs.acs.org.

JA038838K